Organic Electronics 12 (2011) 609–613

Contents lists available at ScienceDirect

Organic Electronics

journal homepage: www.elsevier.com/locate/orgel

The encapsulation of an organic light-emitting diode using organic–inorganic hybrid materials and MgO

Yun Cheol Han [a], Cheol Jang [a], Kuk Joo Kim [a], Kyung Cheol Choi [a,*], KyungHo Jung [b], Byeong-Soo Bae [b]

[a] Department of Electrical Engineering, KAIST, Daejeon, Republic of Korea
[b] Department of Materials Science and Engineering, KAIST, Daejeon, Republic of Korea

ARTICLE INFO

Article history:
Received 9 November 2010
Received in revised form 6 January 2011
Accepted 8 January 2011
Available online 22 January 2011

Keywords:
OLED
Encapsulation
Multi-barrier
Hybrid materials
Sol–gel
Ca test

ABSTRACT

The characteristics of organic–inorganic multi-barriers were investigated in this study. Polymerized cycloaliphatic epoxy hybrid materials (hybrimers), synthesized by a sol–gel method and MgO were used as an organic and inorganic material, respectively. We performed a Ca test at 30 °C and 90% R.H. A multi-barrier of 6 dyads on 100 μm thick PET resulted in a water vapor transmission rate (WVTR) of 4.9×10^{-5} g/m^2 day and optical transmittance of 81.8% in the visible region (350–850 nm). We suggested relatively simple passivation method with a solution process involving an organic material coupled with low temperature deposition of MgO using an electron beam evaporator. Due to the solution process of the organic layer, the OLEDs were passivated without dark spots or an additional protective layer. After driving of 740 h with a constant current source under ambient conditions, a half-life time of 15,000 h was estimated by the stretched exponential decay (SED) model with an initial luminance value $L_0 = 1000$ cd/m^2.

1. Introduction

Organic light-emitting diodes (OLEDs) have great potential for use in next-generation flat-panel displays due to their many advantages, such as their fast response, low power consumption and potential for use with flexible displays. However, reliability issues remain as a major challenge for mass production at present. The organic materials used in OLEDs are very sensitive to oxygen and water vapor. The water vapor transmission rate (WVTR) requirements in organic electronics are stricter than those of any other packaging application [1]. In an OLED, the WVTR must be less than 10^{-6} g/m^2 day. To reduce the weight of the device and realize a full potential of OLEDs, a technology that replaces glass encapsulation is indispensable. Although polymers have been considered as promising candidates for these substrates, the enormously rapid permeation of this setup is known to be a major obstacle [2]. Therefore, a barrier-coating technique is essential before the great potential of OLEDs can be realized. The permeation properties of multi-barriers were discussed by Graff et al. using classical Fickian diffusion models [3]. The effective diffusion path was increased using an alternating layer design.

The lifetime and electroluminescence of OLEDs are directly affected by the formation of non-emitting areas known as dark spots, which accelerate with continuous operation. Various mechanisms of the dark spots have been studied. Crystallization of the organic material by Joule heating and local decomposition of the ITO/organic interface have been reported as possible origins of the dark spots [4,5]. It was also revealed by Liew et al. that cathode delamination is a primary factor in the growth of the dark spots [6]. The growth of the dark spots due to external factors can be blocked by a reliable encapsulation method. Research in relation to the multi-barrier encapsulation

* Corresponding author. Tel.: +82 42 350 3482; fax: +82 42 350 8082.
E-mail address: kyungcc@ee.kaist.ac.kr (K.C. Choi).

1566-1199/$ - see front matter © 2011 Elsevier B.V. All rights reserved.
doi:10.1016/j.orgel.2011.01.007

method has been done in which a vacuum process was utilized. Atomic layer deposition (ALD) and chemical vapor deposition (CVD) have also been shown to provide a high-quality layer [7,8]. However, a vacuum-based deposition process requires considerable time and lowers the price competitiveness. Although a multi-barrier design provides high performance with low WVTR values, encapsulation without dark spots is quite challenging. A protective layer for passivation using a vacuum process is crucial for avoiding damage during the passivation process [9].

In this work, we report a simpler multi-barrier encapsulation method for OLEDs involving the use of a solution process, prepared UV-curable epoxy hybrid materials and the low-temperature deposition of MgO. Directly coated hybrid materials on top of the devices serve as a protective layer in the passivation process. They also function as permeation barrier. A passivated device using the multi-barrier design showed no dark spots. It also demonstrated performance identical to that of glass-lid encapsulation devices.

2. Experimental setup

2.1. Preparation of organic–inorganic hybrid materials

In an earlier study, we prepared a UV-curable epoxy hybrid material (hybrimer) in a sol–gel method [10]. Cycloaliphatic-epoxy oligosiloxane resins were synthesized in a condensation reaction between [2-(3,4-epoxycyclohexyl)ethyl]trimethoxysilane (ECTS, Fluka, USA) and diphenylsilanediol (DPSD, Gelest, USA). Polyethylene glycol methyl ether acetate (PGMEA, Aldrich, USA) and arylsulfonium hexafluorophosphate salt (Aldrich, USA) were used as a solvent and a photo initiator respectively.

The characteristics of the cycloaliphatic-epoxy oligosiloxane resins were also studied [11]. The WVTR value was affected by the siloxane and epoxy network density, and the surface energy of the coating. Higher packing density, greater transparency and lower surface energy were obtained in accordance with increasing the DPSD content of the hybrimer. An optimized hybrimer applicable to the passivation of an OLED was used for the multi-barriers.

2.2. Organic–inorganic multi-barrier coating

In the multi-barrier structure, polymerized cycloaliphatic epoxy hybrid materials (hybrimers) and MgO were used as an organic and inorganic material, respectively. A diluted cycloaliphatic-epoxy oligosiloxane solution with a predetermined amount of solvent (PGMEA) was spin-coated at 2000 rpm for 15 s to create a 1 μm thick layer on 100 μm PET. The coated film was cured by I-line UV light ($\lambda = 365$ nm, optical power density = 11 mW/cm^2) for 360 s. Following this process, thermal curing at 60 °C was conducted in a vacuum chamber for 1.5 h to remove the remaining solvent. 100 nm thick MgO was then deposited using an electron beam evaporator at 2×10^{-6} torr. To prevent the deformation of the film and thermal degradation of the organic materials, a low temperature of 60 °C was maintained, throughout the MgO deposition process. These processes were successively repeated to create the organic–inorganic multi-barrier structure.

2.3. Device fabrication

The OLED was fabricated on a glass substrate coated with indium tin oxide (ITO) in a bottom-emission type. After an O_2 plasma treatment, the 150 nm thick ITO had a sheet resistance of 10 Ω/□. The OLED device had a configuration of ITO(150 nm)/2-TNATA(60 nm)/NPB(30 nm)/Alq$_3$-MADN doped with DCJTB (35 nm)/Alq$_3$(30 nm)/LiF(0.8 nm)/Al(150 nm), wherein 4,4′,4″-tris(2-naphthylphenyl–phenylamino)-triphenylamine (2-TNATA) and *N*,*N*′-bis(1-naphthyl)-*N*,*N*′-diphenyl-1,1′-biphenyl-4,4′-diamine (NPB) independently functioned as a hole injection layer (HIL) and a hole transport layer (HTL). The emitting layer was co-deposited with tris(8-hydroxyquinolinato)aluminum (Alq3) of 20% and 2-methyl-9,10-di(2-naphthyl) anthracene (MADN) of 80% as the co-host materials, and this was doped with 4-(dicyanomethylene)-2-t-butyl-6-(1,1,7,7-tetramethyl-juloli-dyl-9-enyl)-4*H*-pyran (DCJTB) of 2% as a red dopant. Alq$_3$ was subsequently used as an electron transport layer (ETL), and LiF/Al was used as a cathode [12]. Each layer was deposited by a thermal evaporator at 8×10^{-8} torr. Following the fabrication process, the organic–inorganic layers were coated alternatively for passivation via an identical multi-barrier coating method. After the passivation process, silver paste was used to ensure contact. The photograph in Fig. 5 (iii) shows the passivated device.

3. Results and discussion

The WVTR measurements were carried out in a Ca test using the electrical corrosion method involving a Ca sensor at 30 °C and 90% R.H [13]. 100 μm PET was employed as a substrate for the film. A 1.5 cm^2 area of the 250 nm Ca was encapsulated by barrier-coated film with a UV sealant. Al at a thickness of 100 nm was used as an electrode (Fig. 2(a)-(i)). For greater accuracy, a four-point probe system was also utilized during the Ca test. The WVTR value was determined using the following equation:

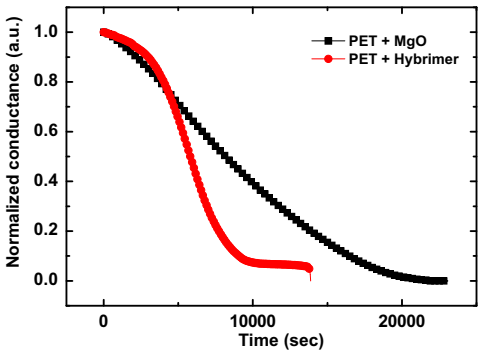

Fig. 1. The permeation test results for the single layer of 1 μm hybrimer and 100 nm MgO on PET substrate.

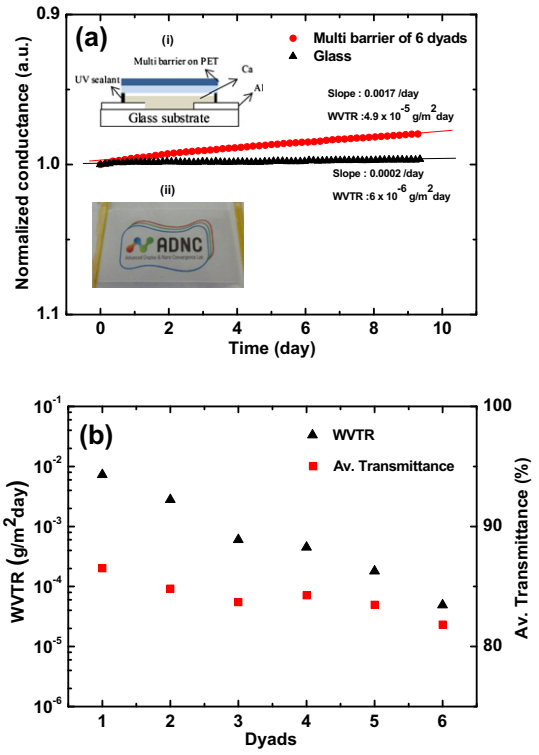

Fig. 2. (a) The results of the Ca test for the 6-dyad multi-barrier on 100 μm PET and glass. Inset: (i) Schematic diagram of the Ca test. (ii) Photograph of a logo image under the 6-dyad multi-barrier on PET. (b) Change in the WVTR and optical transmission (350–850 nm) of the multi-barriers on a 100 μm PET substrate after an increase in the number of dyads.

$$P = -n\left(\frac{1}{R_0}\right)\frac{\mathrm{M}(\mathrm{H_2O})}{\mathrm{M}(Ca)}\delta\rho\frac{l}{b}\frac{d(R_0/R)}{dt}$$

Here, n is the molar equivalent of the degradation reaction, $\mathrm{M}(\mathrm{H_2O})$ and $\mathrm{M}(\mathrm{Ca})$ are the molar masses of H_2O and Ca, respectively. Additionally, δ is the density of the Ca, ρ is the Ca resistivity, l is the length and b is the width of the Ca layer. The slope of the conductance curve R_0/R could be extracted by a Ca test and R_0 is the initial resistance.

Fig. 1 shows the normalized conductance curve of the 1 μm of hybrimer and the 100 nm of MgO on the PET substrate. A WVTR value of 0.79 g/m^2 day for the 1 μm hybrimer and 0.46 g/m^2 day for the single layer of 100 nm MgO was obtained. These WVTR values do not meet requirements of OLED passivation. The WVTR value can be effectively reduced by applying organic–inorganic multi-barriers. Because the permeability is controlled by defects, the diffusion path of oxygen and water vapor can be increased by alternating the layers. To achieve a low WVTR value, each single layer was coated, alternatively, to make a multi-barrier structure.

The Ca test was conducted in accordance with the number of dyads. For the 6-dyad multi-barrier and the glass, the change in the normalized conductance of the Ca sensor is shown in Fig. 2(a). A 1.7% change of the conductance and a WVTR value of 4.9×10^{-5} g/m^2 day were recorded for the multi-barrier. The glass was tested with an identical sealing method. The WVTR value was 6×10^{-6} g/m^2 day with a 0.2% change in the conductance after 10 days. Fig. 2(b) illustrates the performance of the multi-barrier for a set of hybrimer (1 μm)/MgO (100 nm) layers. The WVTR values of multi-barriers, from 1 to 5 dyads, were determined to be 0.0073, 0.0028, 0.0006, 0.00045, and 0.00018 g/m^2 day, respectively. Suppression of the permeation was verified by increasing the number of pairs of layers. The optical transmission of the film was measured using a Shimadzu spectrophotometer (UV-2550). An average transmittance of 81.8% was obtained with 6 dyads on PET in the visible region (350–850 nm) with air used for the baseline. As shown in Fig. 2(a)-(ii), the logo image shows that the transparency of the barrier-coated film is comparable to that of the glass.

Fig. 3 depicts a scanning electron microscope (SEM) image of an individual layer. The cross-section image was taken by a Hitachi instrument (S-4800). A Si wafer was used as the substrate. The film is composed of 100 nm of MgO and 1 μm of hybrimer. Each layer is well defined in the barrier structure. Due to the quality of the spin-coating process, the error range in the thickness of the hybrimer was observed to range from 924 to 1050 nm. However, the effect of the errors did not significantly influence the performance of overall barrier system compared to a 6.6 μm perfect film.

Fig. 4(a) shows the I–V–L characteristics of the multi-barrier passivated OLED and a glass-lid encapsulated device with a desiccant. A 4 mm^2 active area of the devices is defined with an insulator (inset Fig. 4) to eliminate the edge effect by the mask. After encapsulation, the I–V–L results were automatically accumulated by a measurement system with a source meter (Keithley 2400) and a spectrophotometer (TOPCON BM7-A). The maximum luminance of the thin-film passivated OLED showed a luminance value of 33205 cd/m^2 at 24.5 mA according to a dc-current sweep measurement (Fig. 4(b)). These results indicate that no significant differences exist between the two devices.

To evaluate the performance of the multi-barrier, a lifetime test was carried out. The devices were driven by a constant current source of 0.76 mA. The measurements started with an initial luminance value of L_0 = 1000 cd/m^2 under ambient conditions, as shown in Fig. 5. After driving

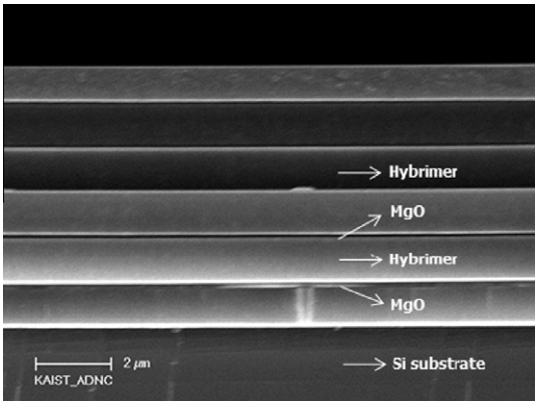

Fig. 3. Cross-sectional SEM image of MgO (100 nm)/hybrimer (1 μm) on a Si substrate.

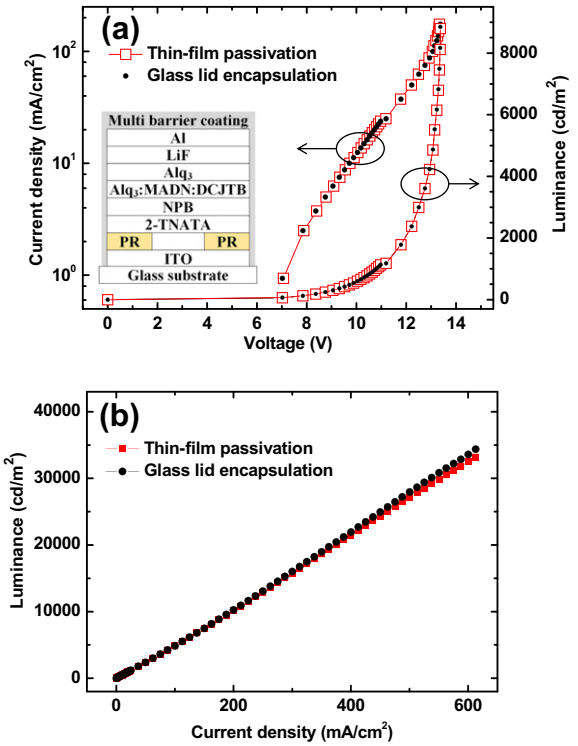

Fig. 4. (a) A comparison of I–V–L characteristics of the encapsulated OLEDs. Inset: Structure of the device. (b) Plot of the luminance versus current density.

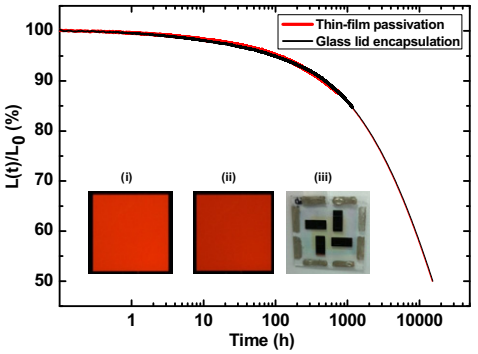

Fig. 5. Half-life time of devices with an initial luminance value $L_0 = 1000$ cd/m^2. The bold lines are the experimental data and the other lines are the exponential fitting data. The inset shows the 4 mm^2 active areas. (i) Before driving, (ii) After driving, (iii) The passivated device. There was no damage during the passivation process and during actual operation.

of 740 h for the thin-film passivated device and at 1182 h for the glass-lid encapsulated device, the lifetime was fitted using the stretched exponential decay (SED) model to consider the half-life time [14,15]. It is known that the luminance of OLEDs decreases exponentially over time. The lifetime was fitted using following equation:

$$L(t) = L_0 \exp\left[-\left(\frac{t}{\tau}\right)^{\beta}\right]$$

In this equation, $L(t)$ is the luminance at time t, L_0 is the initial luminance, and β and τ were obtained from the experimental data. The luminance of the OLEDs decreased to 87.8% of the initial value after operation for 740 h. The lifetime was extrapolated to 15,000 h for the multi-barrier passivation and 15,300 h for the glass-lid encapsulation, respectively, using a constant value for $\beta = 0.556$. In the case of the non-passivated device, the half-decay time was only 5.7 h (not shown in the figure). The microscope image shown in the inset of Fig. 5(i) and (ii) reveals that the OLED did not degrade during the passivation process or during its operation test. The OLED was seriously degraded during the inorganic deposition vacuum process without a protecting layer. When MgO was deposited on top of the device, no light emission was observed. The first layer should serve as a buffer layer during the passivation process. The hybrimer was sufficient to protect the OLED from damage. Due to the solution process of the hybrimer layer, a low-cost and relatively simple OLED passivation process was achieved. The surface roughness of the hybrimer had a RMS value of 0.5 nm in a previous work. We believe that, for the MgO/Hybrimer multi-barrier structure, the MgO surface was planarized in each step. Consequently, the possibility of the formation of the defects and pinholes was reduced effectively at the organic–inorganic interface.

4. Conclusion

We demonstrated the performance of the multi-barriers composed of MgO and UV-curable epoxy hybrid materials (hybrimers). A low WVTR value for the 6-dyad multi-barrier is adequate for encapsulation of the OLED to protect it from water vapor and oxygen. Due to the spin-coated hybrimer layers and the use of MgO deposited at a low temperature, the device was encapsulated without dark spots. The passivated OLED showed stable operation and feasible I–V–L characteristics comparable to those of the glass-lid encapsulated devices. Furthermore, the optimization processes of the barrier structure and composition are practical for application to flexible displays with high transmittance in the visible region. This can be applied to other fields, for instance, to organic thin-film transistors and organic solar cells.

Acknowledgment

This research was supported by Basic Science Research Program through the National Research Foundation of Korea (NRF) funded by the Ministry of Education, Science and Technology (CAFDC-20100009890).

References

[1] P.E. Burrows, G.L. Graff, M.E. Gross, P.M. Martin, M.K. Shi, M. Hall, E. Mast, C. Bonham, W. Bennett, M.B. Sullivan, Displays 22 (2001) 65–69.
[2] M.C. Choi, Y. Kim, C.S. Ha, Progress in Polymer Science 33 (2008) 581–630.
[3] G.L. Graff, R.E. Williford, P.E. Burrows, Journal of Applied Physics 96 (2004) 1840.
[4] S.Y. Kim, K.Y. Kim, Y.H. Tak, J.L. Lee, Applied Physics Letters 89 (2006) 132108.

[5] P. Melpignano, A. Baron-Toaldo, V. Biondo, S. Priante, R. Zamboni, M. Murgia, S. Caria, L. Gregoratti, A. Barinov, M. Kiskinova, Applied Physics Letters 86 (2005) 041105.
[6] Y.F. Liew, H. Aziz, N.X. Hu, H.S.O. Chan, G. Xu, Z. Popovic, Applied Physics Letters 77 (2000) 2650.
[7] A.P. Ghosh, L.J. Gerenser, C.M. Jarman, J.E. Fornalik, Applied Physics Letters 86 (2005) 223503.
[8] K. Yamashita, T. Mori, T. Mizutani, Journal of Physics D: Applied Physics 34 (2001) 740.
[9] F.L. Wong, M.K. Fung, S.L. Tao, S.L. Lai, W.M. Tsang, K.H. Kong, W.M. Choy, C.S. Lee, S.T. Lee, Journal of Applied Physics 104 (2008) 014509.
[10] K.H. Jung, B.S. Bae, Journal of Applied Polymer Science 108 (2008) 3169–3176.
[11] K.H. Jung, J.Y. Bae, S.J. Park, S.H. Yoo, B.S. Bae, Journal of Materials Chemistry (2010).
[12] Y.G. Lee, H.N. Lee, S.K. Kang, T.S. Oh, S. Lee, K.H. Koh, Applied Physics Letters 89 (2006) 183515.
[13] R. Paetzold, A. Winnacker, D. Henseler, V. Cesari, K. Heuser, Review of Scientific Instruments 74 (2003) 5147.
[14] C. Fery, B. Racine, D. Vaufrey, H. Doyeux, S. Cina, Applied Physics Letters 87 (2005) 213502.
[15] B. Racine, C. Fery, A. Bettinelli, H. Doyeux, S. Cina, T.R.D. France, Organic Thin-Film Electronics 34 (1) (2005) 12–34.